SUPPLEMENTARY INFORMATION

Mechanisms of recalcitrant fucoidan breakdown in marine Planctomycetota

Carla Pérez-Cruz[1,#], Alicia Moraleda-Montoya[2,#], Raquel Liébana[1,#], Oihana Terrones[3], Uxue Arrizabalaga[1], Mikel García-Alija[2], Maier Lorizate[3], Ana Martínez Gascueña[2], Isabel García-Álvarez[4], Jon Ander Nieto-Garai[3], June Olazar-Intxausti[3], Bárbara Rodríguez-Colinas[4], Enrique Mann[5], José Luis Chiara[5], Francesc-Xabier Contreras[3,6,7,*], Marcelo E. Guerin[8,*], Beatriz Trastoy[2,7,*] and Laura Alonso-Sáez[1,*]

[1]AZTI, Marine Research, Basque Research and Technology Alliance (BRTA), Sukarrieta, Spain.
[2]Structural Glycoimmunology Laboratory, Biobizkaia Health Research Institute, 48903 Barakaldo, Spain.
[3]Department of Biochemistry and Molecular Biology, Faculty of Science and Technology, University of the Basque Country, Leioa, E-48940, Spain.
[4]Facultad de Ciencias Experimentales, Universidad Francisco de Vitoria, Pozuelo de Alarcón, 28223 Madrid, Spain.
[5]Instituto de Química Orgánica General (IQOG-CSIC), Juan de la Cierva 3, 28006 Madrid, Spain.
[6]Instituto Biofisika (UPV/EHU, CSIC), University of the Basque Country, Leioa, E-48940, Spain.
[7]Ikerbasque, Basque Foundation for Science, 48009 Bilbao, Spain.
[8]Structural Glycobiology Laboratory, Department of Structural and Molecular Biology; Molecular Biology Institute of Barcelona (IBMB), Spanish National Research Council (CSIC), Barcelona Science Park, c/Baldiri Reixac 4-8, Tower R, 08028 Barcelona, Catalonia, Spain.

[#]These authors contributed equally

*To whom correspondence should be addressed: Francesc-Xabier Contreras, [4]Department of Biochemistry and Molecular Biology, Faculty of Science and Technology, University of the Basque Country, 48940 Leioa, Spain, xabier.contreras@ehu.eus; Marcelo E. Guerin, Structural Glycobiology Laboratory, Department of Structural and Molecular Biology; Molecular Biology Institute of Barcelona (IBMB), Spanish National Research Council (CSIC), mrccri@ibmb.csic.es; Beatriz Trastoy, Structural Glycoimmunology Laboratory, Biobizkaia Health Research Institute, Cruces University Hospital, 48903 Barakaldo, Bizkaia, Spain, beatriz.trastoy@gmail.com; Laura Alonso-Sáez, AZTI, Marine Research, Basque Research and Technology Alliance (BRTA), 48395 Sukarrieta, Spain, lalonso@azti.es.

Table of Contents

1. Supplementary Tables

Supplementary Table 1. Carbohydrate composition of selected fucoidans.

Brown algal fucoidan	% (w/w) building block	Source	Major linkage pattern	References
Fucus vesiculosus	45% fucose 3% galactose 1% mannose 2% xylose 2% glucuronic acid 26% sulfate	Sigma-Aldrich	alternating 3- and 4-linked α-L-fucopyranose (Homofucan)	[1,2]
Undaria pinnatifida	27% fucose 25% galactose 26% sulfate	Sigma-Aldrich	alternating fucose – galactose backbone linked together via 1,3 glycosidic bonds (Heterofucan)	[3–5]
Cladosiphon okamuranus	40% fucose 2% galactose 1% xylose 15% glucuronic acid 9% galacturonic acid 13% sulfate	Biosynth	repetitions of a-(1-3)-L-fucopyranose with with 4-O-sulfation and α-1,2-linked glucuronic acid branches (Homofucan)	[1]
Ecklonia maxima	17% fucose 15% galactose 3% mannose 2% xylose 9% glucuronic acid 18% sulfate	Biosynth	alternating 3- and 4-linked α-L-fucopyranose (Homofucan)	[1]
Macrocystis pyrifera	24% fucose 3% galactose 1% mannuronic acid 2% glucuronic acid 26% sulfate	Biosynth	Not defined	[1]

Supplementary Table 2. X-ray data collection and refinement statistics.

	Rho5174	**PbFucA-1**	**PbFucA-2**	**PbFucA-3**
PDB code	9F9V	8RG3	8RG4	8RG5
Beamline	BL13 XALOC	I24 (DLS)	I04 (DLS)	I04 (DLS)
Wavelength (Å)	0.9792	0.9795	0.9795	0.9795
Resolution range (Å)	36.45 - 1.57 (1.626 - 1.57)	91.42 – 2.5 (2.60-2.5)	9.99 - 1.40 (1.45-1.40)	28.99-2.18 (2.26 – 2.18)
Space group	P 1	P 1 21 1	P 21 21 21	P 41 21 2
Unit cell (Å)	44.39 62.11 66.9 68.83 88.34 78.92	91.841 81.90 160.31 90 95.5 90	50.983 84.87 90.344 90 90 90	139.30 139.30 104.69 90 90 90
Total reflections	306199 (29824)	460909 (45579)	1007201 (89749)	140999 (139461)
Unique reflections	87100 (8585)	82173 (8083)	76431 (7135)	54121 (5322)
Multiplicity	3.5 (3.5)	5.6 (5.6)	13.2 (12.6)	27.0 (26.2)
Completeness (%)	95.43 (94.14)	99.87 (99.75)	99.02 (93.64)	99.93 (100)
Mean I/sigma(I)	13.86 (1.48)	12.23 (1.92)	19.63 (3.34)	20.91 (4.62)
Wilson B-factor (Å^2)	22.42	38.15	14.30	30.91
R-merge	0.05393 (0.8413)	0.1382 (0.9698)	0.07903 (0.7331)	0.1472 (0.7482)
R-meas	0.0285 (0.4449)	0.1536 (1.073)	0.08231 (0.7642)	0.150 (0.7628)
CC1/2	0.999 (0.631)	0.994 (0.675)	0.999 (0.872)	0.999 (0.956)
CC*	1 (0.88)	0.999 (0.898)	1.0 (0.965)	1.0 (0.989)
Reflections used in refinement	87082 (8585)	82142 (8080)	76416 (7127)	54116 (5325)
Reflections used for R-free	4354 (429)	1997 (197)	3837 (324)	2641 (262)
R-work	0.2087 (0.3254)	0.2275 (0.3591)	0.1433 (0.1676)	0.2040 (0.2027)
R-free	0.2328 (0.3564)	0.2624 (0.3956)	0.1635 (0.2175)	0.2459 (0.2329)
CC(work)	0.951 (0.738)	0.952 (0.750)	0.969 (0.929)	0.938 (0.935)
CC(free)	0.938 (0.669)	0.941 (0.606)	0.962 (0.918)	0.919 (0.917)
Number of non-hydrogen atoms	6193	16917	3311	5795
macromolecules	5794	16739	2960	5602
ligands	65	12	20	128
Protein residues	720	2134	356	704
RMS(bonds) (Å)	0.004	0.012	0.008	0.011
RMS(angles) (º)	0.69	1.20	1.01	0.98
Ramachandran favored (%)	98.31	96.61	97.46	97.42
Ramachandran allowed (%)	1.69	3.11	2.54	2.44
Ramachandran outliers (%)	0.00	0.28	0.00	0.14
Rotamer outliers (%)	0.00	1.24	0.00	0.36
Clashscore	2.90	5.99	0.85	3.09
Average B-factor (Å^2)	27.78	49.93	17.21	37.12
macromolecules	27.34	50.02	16.11	37.16
ligands	35.96	40.06	25.08	39.85
solvent	33.97	41.78	26.57	34.41

Statistics for the highest-resolution shell are shown in parentheses

Supplementary Table 3. Structure weighted sequence comparison of GH168 endo-fucoidanases from *Planctomycetes* bacterium *K23_9* (PbFucA, PbFucAG3, PbFucA70*), *W. fucanilytica* CZ1127^{T} (Fun168A and Fun168D) and strains 892 and 913. 40% amino acid sequence identity or higher is highlighted in orange.

r.m.d.s in Å (aligned residues)

	PbFucA	PbFucAG3	PbFucA70	Fun168A	Fun168D	Rho5174	892_06282	892_06289	913_01189	913_05635	
PbFucA		1.018 (191)	1.096 (195)	1.010 (225)	1.020 (256)	1.072 (268)	0.963 (228)	1.104 (248)	1.135 (246)	1.075 (256)	**PbFucA**
PbFucAG3	21.70		1.062 (134)	1.087 (173)	0.920 (175)	1.167 (188)	1.218 (171)	0.918 (178)	0.989 (176)	1.151 (193)	**PbFucAG3**
PbFucA70	22.58	13.94		1.134 (166)	1.160 (156)	1.056 (184)	1.049 (179)	1.089 (136)	1.117 (151)	1.066 (184)	**PbFucA70**
Fun168A	31.67	17.43	15.93		1.014 (187)	0.845 (241)	0.683 (323)	1.076 (196)	1.059 (197)	0.892 (250)	**Fun168A**
Fun168D	23.17	20.11	14.15	18.63		1.088 (213)	1.074 (185)	0.874 (287)	0.782 (294)	1.070 (220)	**Fun168D**
Rho5174	36.07	20.67	18.99	33.52	24.86		0.857 (250)	1.146 (214)	1.104 (215)	0.411 (347)	**Rho5174**
892_06282	31.67	19.24	20.70	64.43	24.78	34.99		1.174 (208)	1.149 (190)	0.851 (247)	**892_06282**
892_06289	28.45	19.83	19.26	24.08	40.79	25.50	25.36		0.779 (315)	1.082 (190)	**892_06289**
913_01189	26.10	18.86	17.71	24.29	45.43	26.29	24.78	48.86		1.052 (204)	**913_01189**
913_05635	36.36	20.56	19.72	32.78	23.61	75.98	33.82	27.48	27.43		**913_05635**
	PbFucA	**PbFucAG3**	**PbFucA70**	**Fun168A**	**Fun168D**	**Rho5174**	**892_06282**	**892_06289**	**913_01189**	**913_05635**	

Amino acid sequence identity (%)

Supplementary Table 4. List of total GHs and SAs from strains 892 and 913 arranged in fucoidan PULs, and expressed at proteomic level. The number of proteins detected by proteomics and induced in at least one fucoidan source are specified.

	892			913		
List of GHs and Sas potentially involved in fucoidan degradation	Nº of GH and SAs arranged in Fucoidan PULS	Nº of GH and SAs detected	Nº of GH and SAs induced	Nº of GH and SAs arranged in Fucoidan PULS	Nº of GH and SAs detected	Nº of GH and SAs induced
GH29	13	**9**	**6**	15	**5**	**4**
GH95	5	**4**	**3**	5	**1**	**1**
GH141	3	**1**	**0**	5	**2**	**2**
GH141+GH168	1	**1**	**1**	0	**0**	**0**
GH107	0	**0**	**0**	1	**1**	**1**
GH168	2	**1**	**1**	2	**1**	**1**
Total GH	**24**	**16**	**11**	**28**	**10**	**9**
S1_14	6	**1**	**1**	6	**0**	**0**
S1_15	2	**1**	**1**	8	**1**	**1**
S1_16	4	**1**	**0**	5	**1**	**1**
S1_17	3	**3**	**1**	6	**1**	**1**
S1_22	1	**1**	**0**	2	**2**	**1**
S1_25	2	**1**	**1**	4	**0**	**0**
Total SAs	**18**	**8**	**4**	**31**	**5**	**4**
Total enzymes	**42**	**24**	**15**	**59**	**15**	**13**

Supplementary Table 5. Genome assembly statistics of *Planctomycetota* strains 892 and 913.

Genome	contigs (>= 0 bp)	contigs (>= 1,000 bp)	Total length (>= 1,000 bp)	N50	N90	auN	L50	L90	N's per 100 kbp	ORF nr.
892	31	1	9,109,604	9,109,604	9,109,604	9,109,604	1	1	0	6,830
913	53	1	7,962,739	7,962,739	7,962,739	7,962,739	1	1	0	6,015

2. Supplementary note 1

The overall structure of PbFucA from *Planctomycetes bacterium* K23_9

To elucidate the structural determinants that govern the substrate specificity of the GH168 family of endo-fucosidases we crystallized PbFucA from *Planctomycetes* bacterium K23_9 in three crystal forms, PbFucA-1, PbFucA-2 and PbFucA-3 corresponding to the space groups, $P12_11$ at 2.2 Å (PDB code 8RG3), $P2_12_12_1$ at 1.4 Å (PDB code 8RG4) and $P4_12_12$ at 2.1 Å resolution (PDB code 8RG5), respectively (Supplementary Figs. 5 and 12, Supplementary Table 2; see Methods section for further details). The overall protein scaffold and the conformation of the three crystal forms were essentially preserved (r.m.s.d. of 0.392 Å for 353 aligned residues, PbFucA-1 and PbFucA-2; r.m.s.d. of 0.368 Å for 353 aligned residues, PbFucA-1 and PbFucA-3; r.m.s.d. of 0.392 Å for 353 aligned residues, PbFucA-2 and PbFucA-3; Supplementary Fig. 13a). We decided to use the PbFucA-2 crystal form for our description since it displays the highest resolution. The high quality of the electron density maps allowed the trace of residues 37–392 (Supplementary Fig. 12). PbFucA contains (i) a catalytic domain adopting a conserved $(\beta/\alpha)_8$ barrel topology (residues 35-359) and (ii) a small C-terminal subdomain (residues 360-392) comprising a β-sheet conformation composed of 4 antiparallel β-strands, with an overall size of 58 Å × 49 Å × 28 Å (Supplementary Fig. 13). The $(\beta/\alpha)_8$ barrel is a conserved protein fold consisting of eight α-helices and eight parallel β-strands that alternate along the peptide backbone. The catalytic domain and the C-terminal subdomain interact with each other through an extensive contact area of ca. 1168 $Å^2$, representing 8% of the total accessible surface of the isolated domains (Supplementary Fig. 13). A large groove runs at the center of the catalytic domain, containing the active site of the enzyme. This groove is surrounded by the loops connecting β1–α1 (loop 1; residues 55-62, light blue), β2–α2 (loop 2; residues 79–89, dark red), β3–α3 (loop 3; residues 114–158, green), β4–α4 (loop 4; residues 184–199, yellow), β5–β6 (loop 5; residues 230–236, pink), β6–α5 (loop 6; residues 254–263, orange), β7–α6 (loop 7; residues 290–296, dark blue), and β8–α7 (loop 8; residues 336–362, khaki; Supplementary Fig. 13).
We unambiguously identified an ethylene glycol molecule in the central groove of the PbFucA structure corresponding to space groups $P2_12_12_1$ and $P4_12_12$ and in two molecules corresponding to the space group P1211. This ethylene glycol molecule is placed near the predicted catalytic residues D184 and E254 (Supplementary Fig. 13a,d), likely mimicking the position of a Fuc (-1) residue. These residues were identified based on sequence alignment with the two biochemically characterized members of the GH168 family, Fun168A [7] and Fun168D [8] from W. fucanilytica CZ1127T, sharing 31% and 23% sequence identity with PbFucA, respectively (Supplementary Fig. 14a). The O2 atom of the ethylene glycol molecule interacts by hydrogen bonds with the side chain of D184 and makes additional polar and hydrophobic interactions with H53, E79, Y113, N230, E254, and Y338 (Supplementary Fig. 13d).

A search for structural homologues using the DALI server [9] revealed that PbFucA shows structural similarity to other GHs (Supplementary Fig. 14), including: (i) Fun168A from *W. fucanilytica* CZ1127^T, an endo-a-1,3-fucanase that belongs to the GH168 family (PDB code 8YA6, Z-score of 42, r.m.s.d. value of 1.9 Å for 369 aligned residues; 37% identity), (ii) *Tm*GalA, an α-galactosidase from *Thermotoga maritima* that belongs to the GH36 family [10]; PDB code 5M1I, Z-score of 18.2, r.m.s.d. value of 3.9 Å for 288 aligned residues; 14% identity), and (iii) LaMel36A, an α-galactosidase from *Lactobacillus acidophilus NCFM* that also belongs to the GH36 family [11]; PDB code 2XN1, Z-score of 16.7, r.m.s.d. value of 3.9 Å for 278 aligned residues; 11% identity).

3. Supplementary Figures

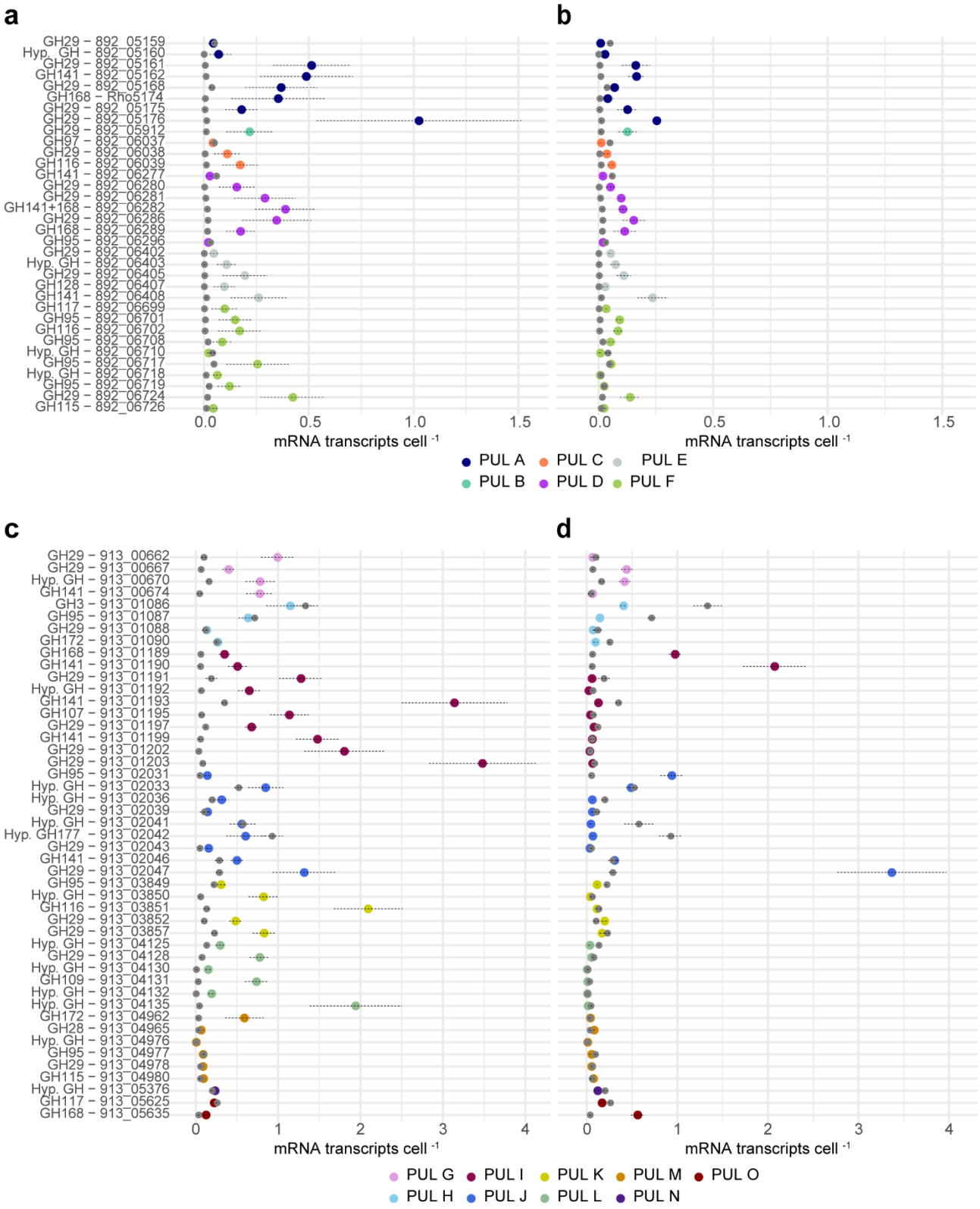

Supplementary Fig. 1 | Gene expression at mRNA level of glycosyl hydrolases in the different Fucoidan Polysaccharide Utilization Loci (PULs) in strain 892 (a, b) and 913 (c, d). Transcripts per cell of GHs in the different fucoidan PULs (highlighted in different colours) when growing on fucoidan from *Fucus vesiculosus* (a and c) and *Undaria pinnatifida* (b and d) as compared to laminarin (dark gray dots in each panel). Data represent means and error bars show the standard deviation derived from three biologically independent experiments. GH: glycosyl hydrolase; Hyp: hypothetical.

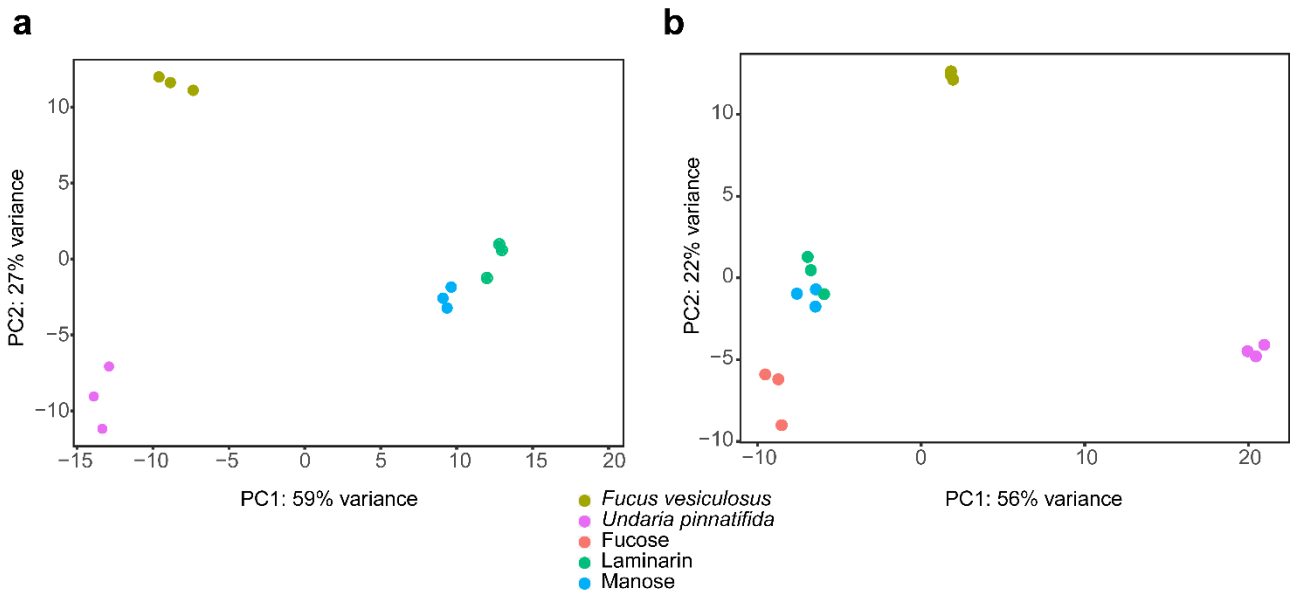

Supplementary Fig. 2 | Principal component analysis of the RNA-seq expression datasets in strain 892 (a) and 913 (b). Principal component analysis (PCA) of the variance stabilized transformed (vst) RNA-seq expression data showing distinct clustering of the samples depending on the carbon source, derived from three biologically independent experiments.

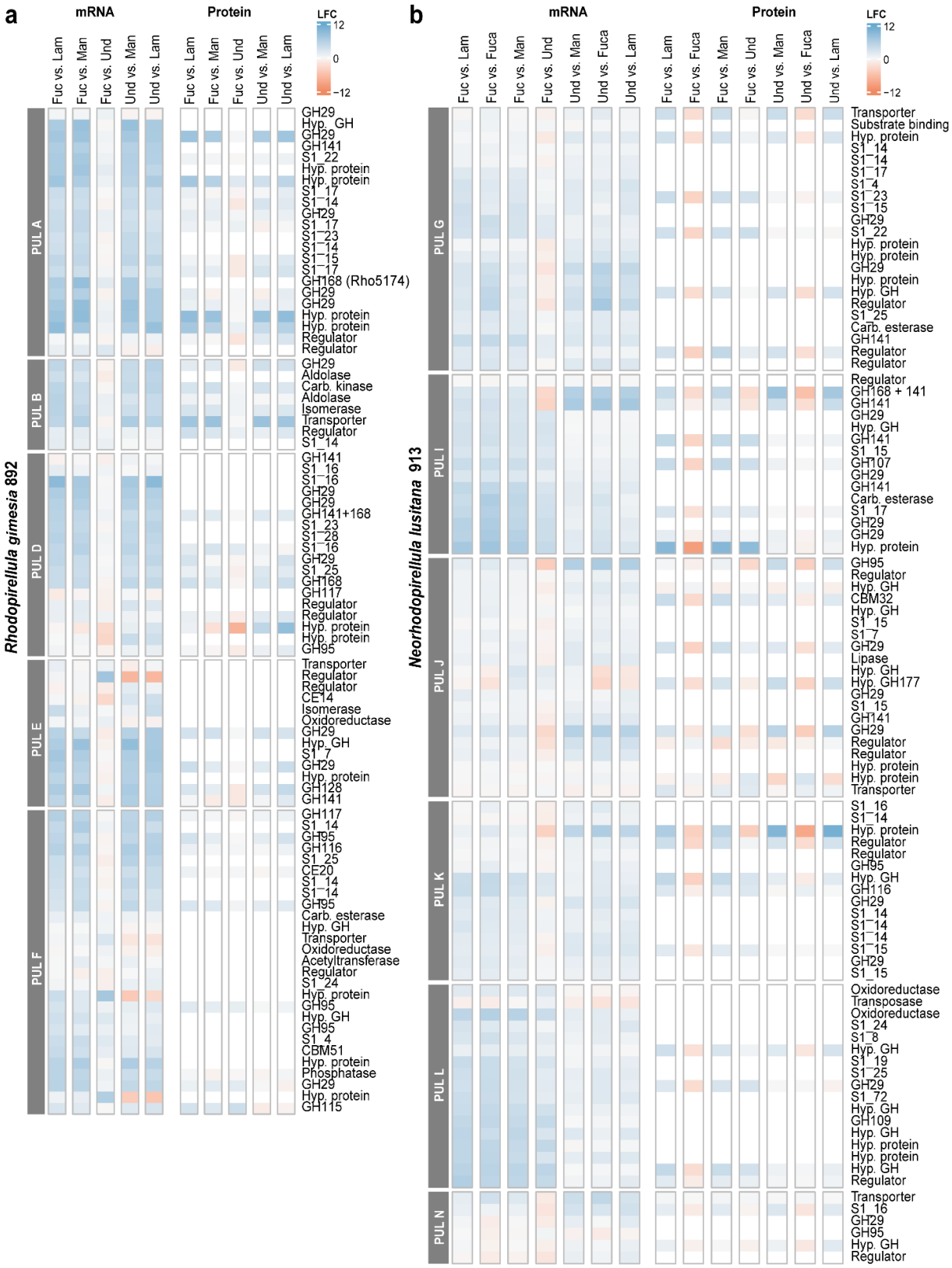

Supplementary Fig. 3 | Differential gene expression at mRNA and protein level in the identified fucoidan PULS, in the genomes of 892 (a) and 913 (b). Log_2-fold changes (LFC) of mRNA and protein expression data based on pairwise comparisons between different carbon sources. Color scale indicates upregulation (blue) or downregulation (red) of transcripts or proteins in the indicated fucoidan vs. other carbon sources. Expression values were quantified in three biologically independent replicates. Only PULs where fucosidases were expressed at the protein level are shown. Fuc: fucoidan from *Fucus vesiculosus*; Und: fucoidan from *Undaria pinnatifida*; Lam: laminarin; Man: mannose; Fuca; fucose. Data are shown as average estimates of three independent biological experiments.

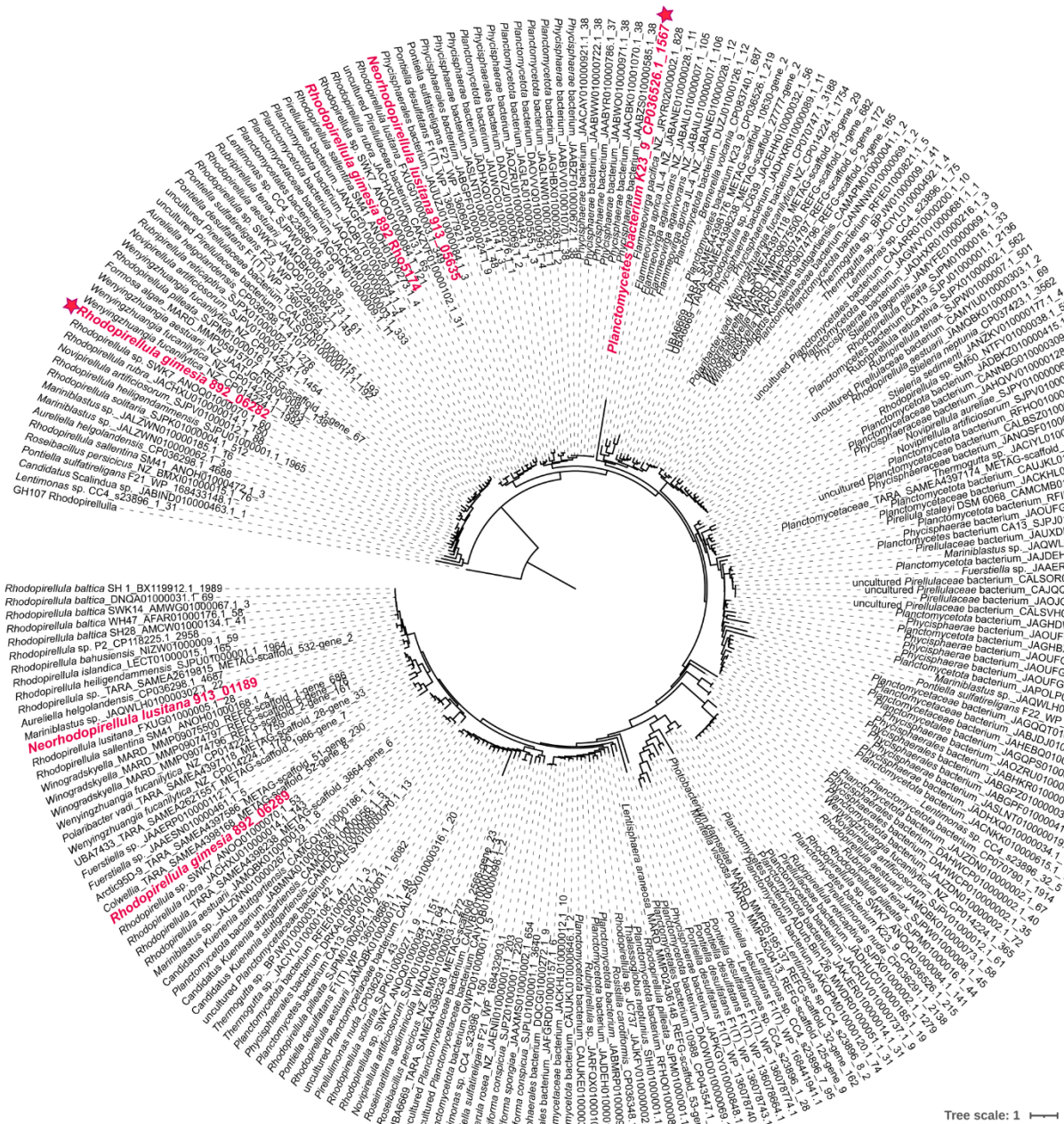

Supplementary Fig. 4 | Phylogenetic tree of GH168 homologues. Maximum likelihood phylogenetic tree of GH168 homologue amino acid sequences from all available Planctomycetota genomes at NCBI, selected genomes of Bacteroidota and Verrucomicrobiota, and environmental sequences found in *The Ocean Microbiomics Database* gene catalogue [12].

a

MHHHHHHENLYFQGSGMPAFSWDTVPVYLHFGSPTKMTNEQVQTAARLSNFICLEKAHGRTTDREHPERIAAEDAQ
RIKTANPDAKVLMYWNTLIAWPFTSYNSDFAETHPENWTLRDRSTGEPLLKAMHGSTPYQYNLLNPDVRKWWADTIG
GAVNEFNFDGVFMDAVSQSKRPLWLQKGWGLDKADELDAAAVDMMRQTKAIIGNNRLLIYNGFRSKSGGPDNNAAA
GTEFLPYSDGAQIEHFDQLSSITKEDMVAYWKMAATAAKDNKIVLYKAWPDHDINWLNRKFMSQSPAKKEAFAREKITY
PLACYLIGAEENSYFCYGWGYGIDDGQLVDYPEYRKPLGAPKSRARRTGWIFRREFEHANVAVDLENRKARIQWLRD

b

MHHHHHHENLYFQGSGDESHYPEFSWDTVPIAFHFGKSQGLLTKEEAEFVATRSNFICLEKGHATRTHGTTEAGIEA
EARQLKNLNPKMKVIFYWNTFLDYSMFAAHKEYAKHPQWWLRTTTGELDRKKGQLMRYDLSNAEFRNWWTNVAAK
AVVDGTCDGVFMDAFPQIASQANRKLWGDEKFEAIQQGLQDIIQETRQKIGDDKLIVYNGIRSTPDWSAGFDFAEYT
DAAMIEHFGHFQSASKETMLRDILEMQRAAKAGKIVVLKGWAGFTFIDDQAMRKPLTQKRRVAKDSLKFPLACFLAG
AQENCYFIYN

c

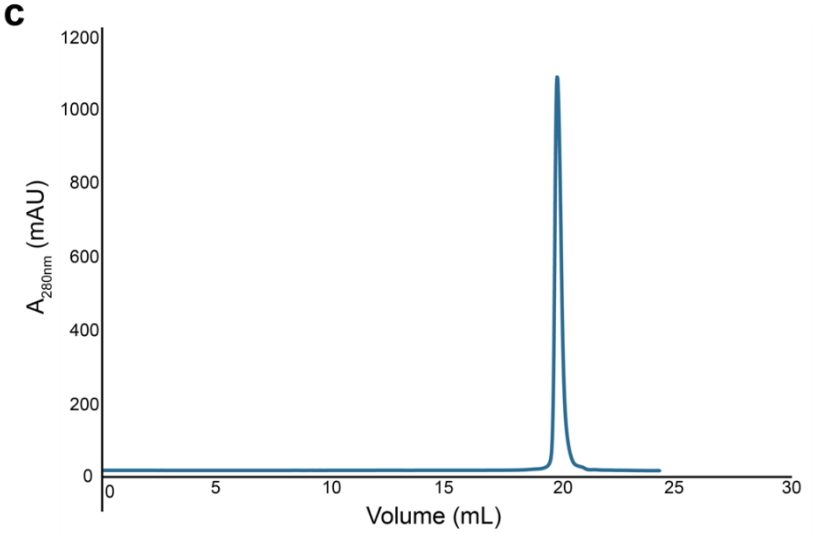

d

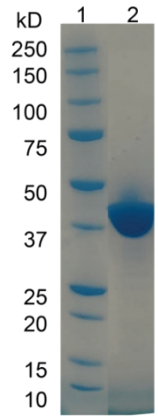

e

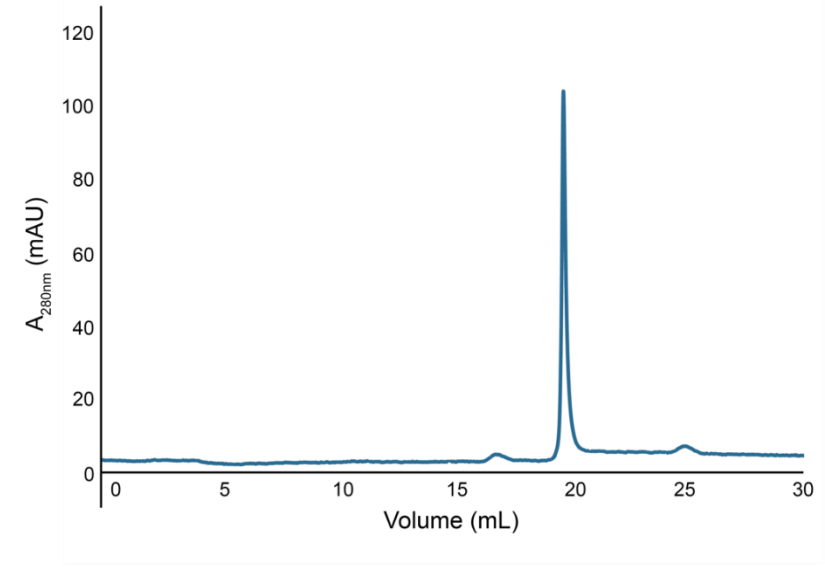

f

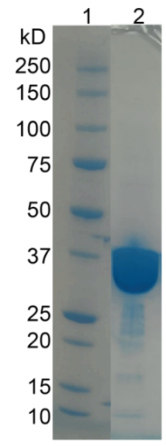

Supplementary Fig. 5 | Recombinant production of Rho5174 and PbFucA. a-b Schematic representation of Rho5174 (**a**) and PbFucA (**b**) from *Planctomycetes bacterium K23_9* amino acid sequence. The catalytic residues D152 and E228, are highlighted in yellow. The His-tag is colored in light blue and the Tobacco Etch Virus Protease (TEV) cutting site is shown in pink. **c-d** Pre-crystallization SEC purification (**c**) and SDS-PAGE (**d**) analysis of Rho5174. **e-f** Pre-crystallization SEC purification (**e**) and SDS-PAGE (**f**) analysis of PbFucA. This experiment was repeated three times independently with similar results.

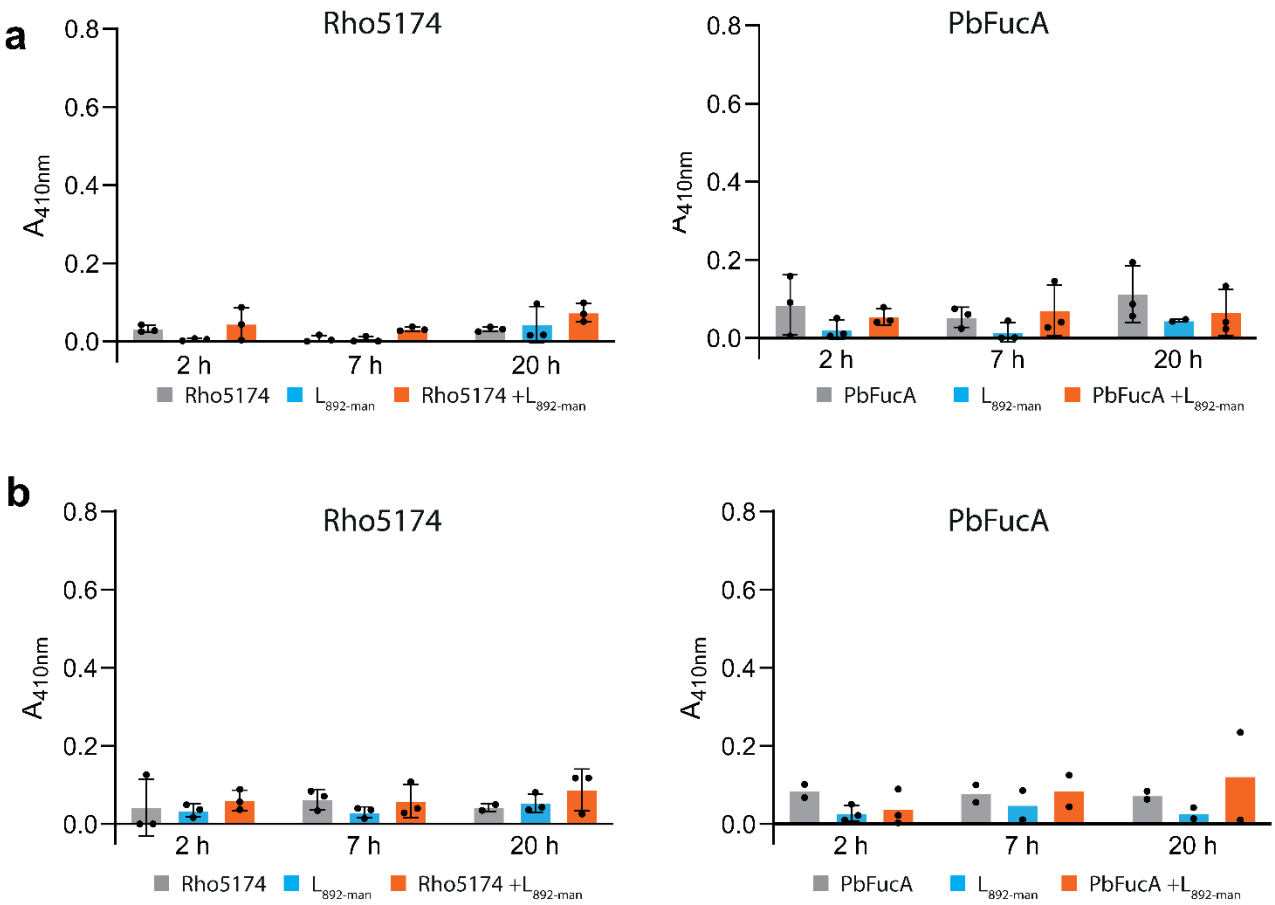

Supplementary Fig. 6| Hydrolytic activity of PbFucA, Rho5174 and strain 892 lysates grown in mannose. a Hydrolytic activity of Rho5174 (left) and PbFucA (right), strain 892 lysate grown in mannose ($L_{892\text{-man}}$) and the combination of enzyme and lysate against fucoidan from *F. vesiculosus.* **b** Hydrolytic activity of Rho5174 (left), PbFucA (right), $L_{892\text{-man}}$ and combination of enzymes and lysate against fucoidan from *U. pinnatifida*. The hydrolytic activity of the enzymes, strain 892 lysate, and the combination of enzyme and lysate are colored in grey, blue, and orange, respectively.

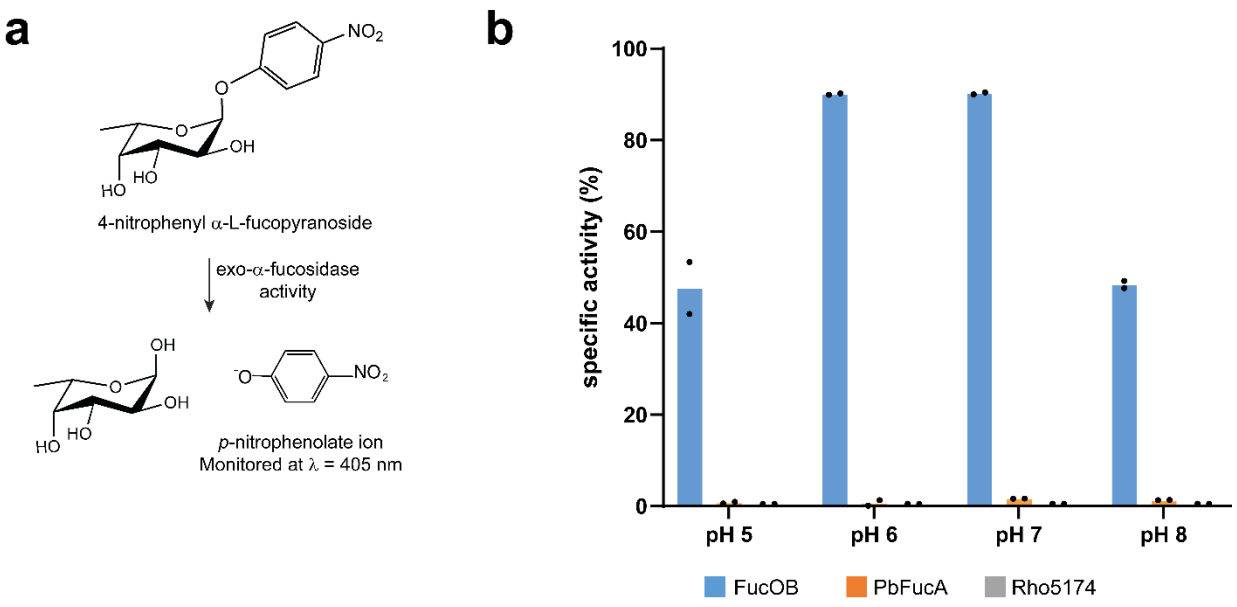

Supplementary Fig. 7 | PbFucA and Rho5174 *exo*-fucosidase activity assays. a Schematic representation of exo-fucosidase activity assay using 4-nitrophenyl α-L-fucopyranoside. **b** Exo-fucosidase activity of PbFucA (orange) and Rho5174 (gray) and the positive control exo-α-1,2-fucosidase FucOB[13] (blue).

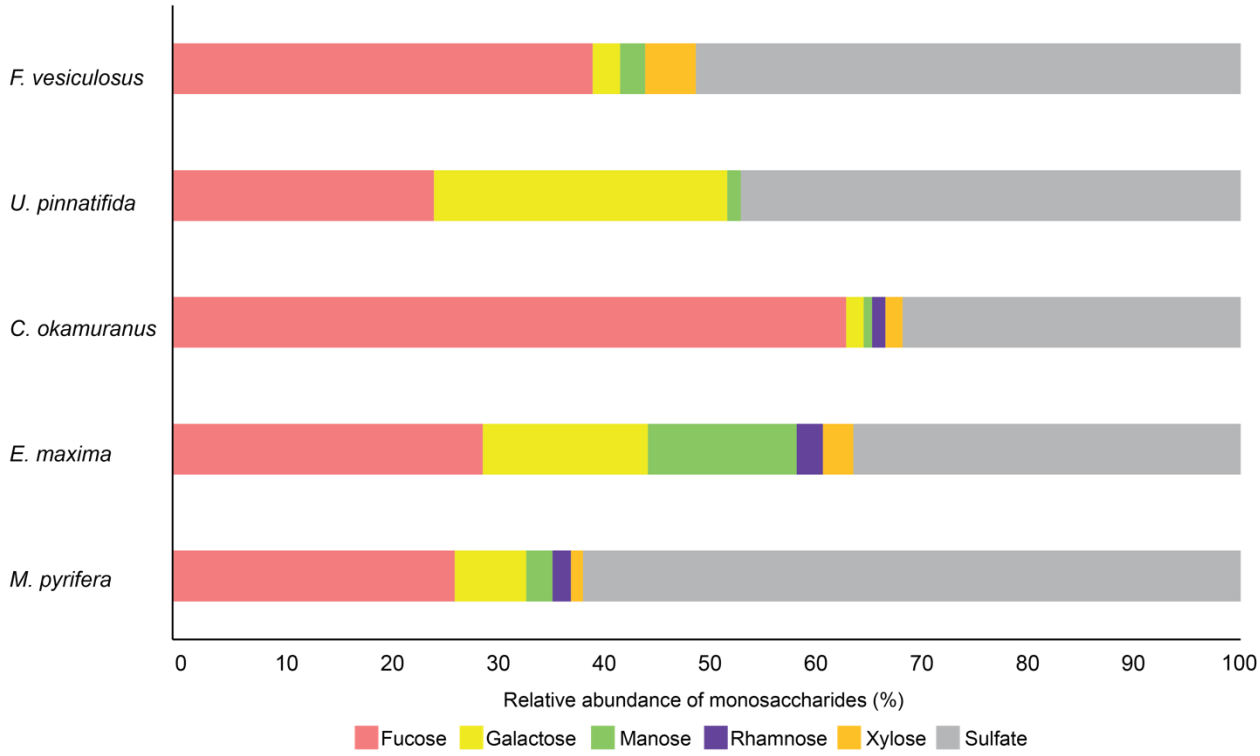

Supplementary Fig. 8| Overview of the monosaccharide and sulfate composition of the fucoidans analysed in this study. Mean relative abundance of monosaccharides and sulfate conformation from analytical triplicates.

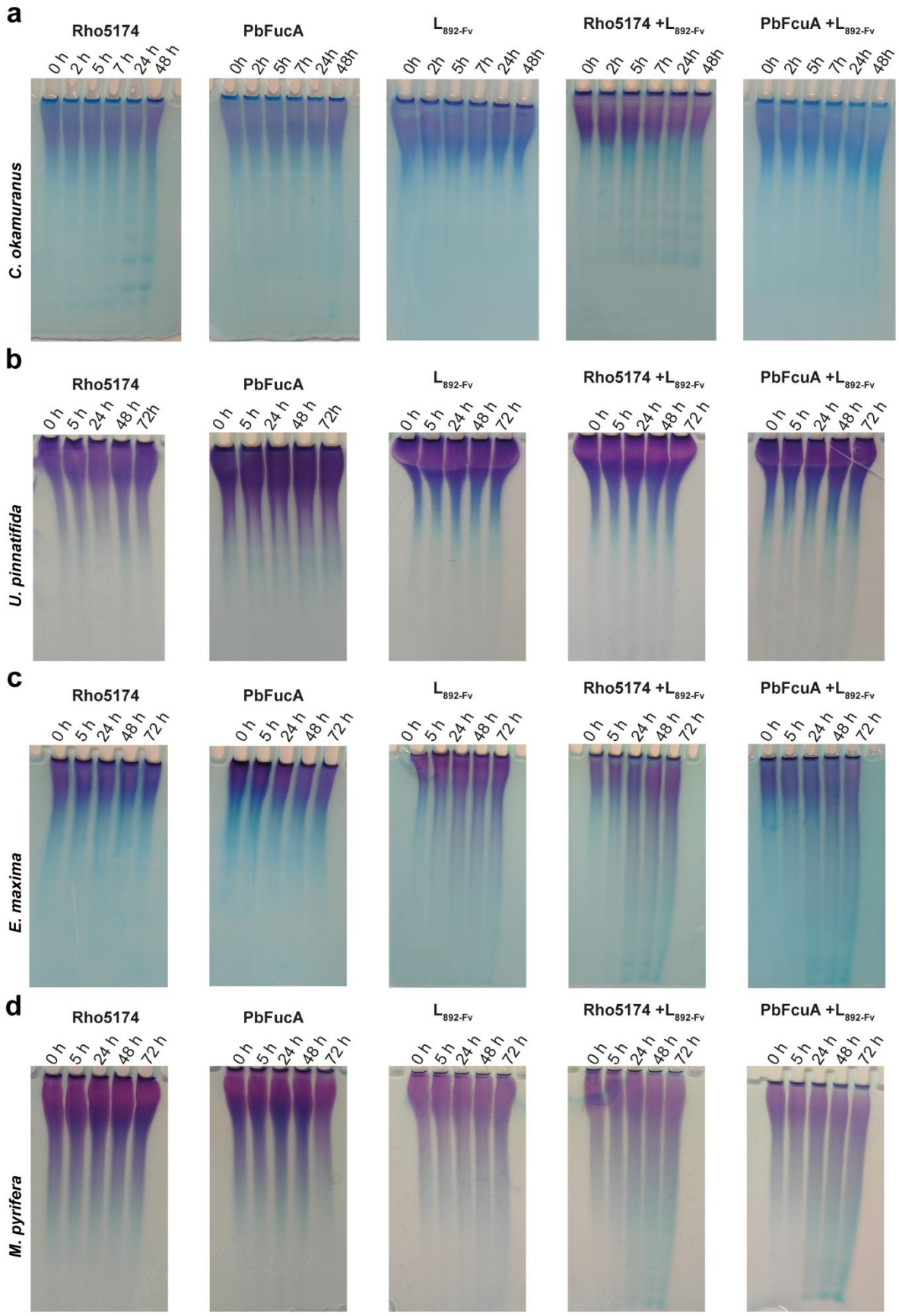

Supplementary Fig. 9 | Hydrolytic activity of PbFucA, Rho5174 and strain 892 lysate against fucoidan from various brown algae species. a-d C-PAGE analysis of the hydrolytic activity of Rho5174 and PbFucA, strain 892 lysate grown in *F. vesiculosus* ($L_{892\text{-}Fv}$) and the combination of enzymes and lysate against fucoidan from *C. okamuranus* (**a**), *U. pinnatifida* (**b**), *E. maxima* **(c)** and *M. pyrifera* (**d**).

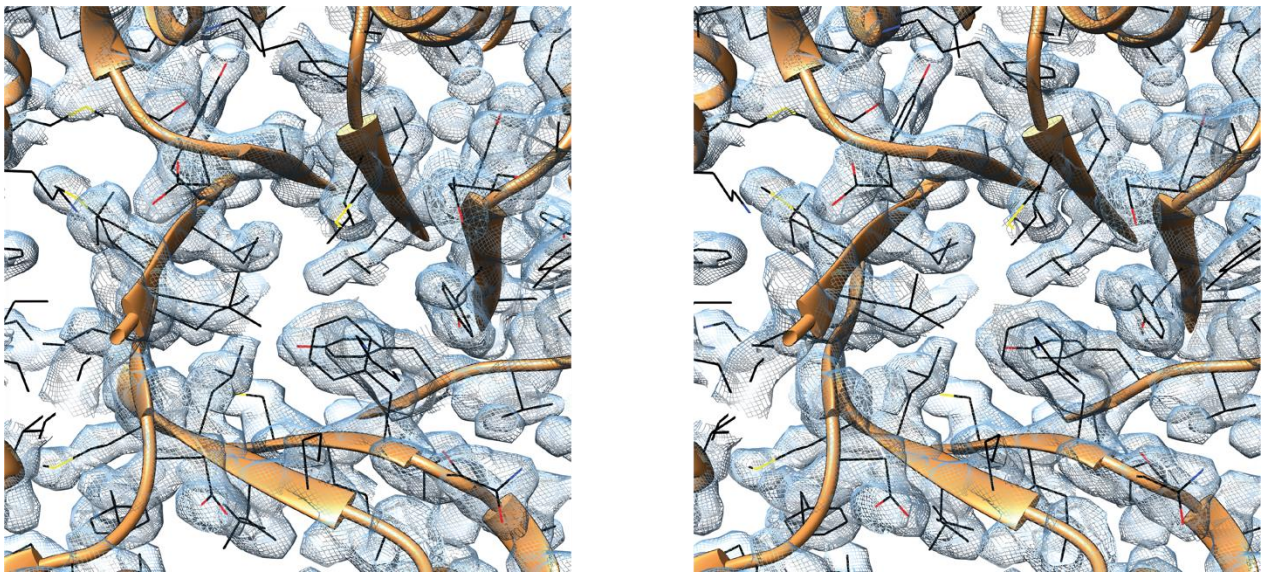

Supplementary Fig. 10 | Electron density maps of the refined Rho1574 X-ray crystal structures. Final electron density maps (2mFo-Dfc contoured at 1σ) corresponding to 892_01574 (PDB code 9F9V).

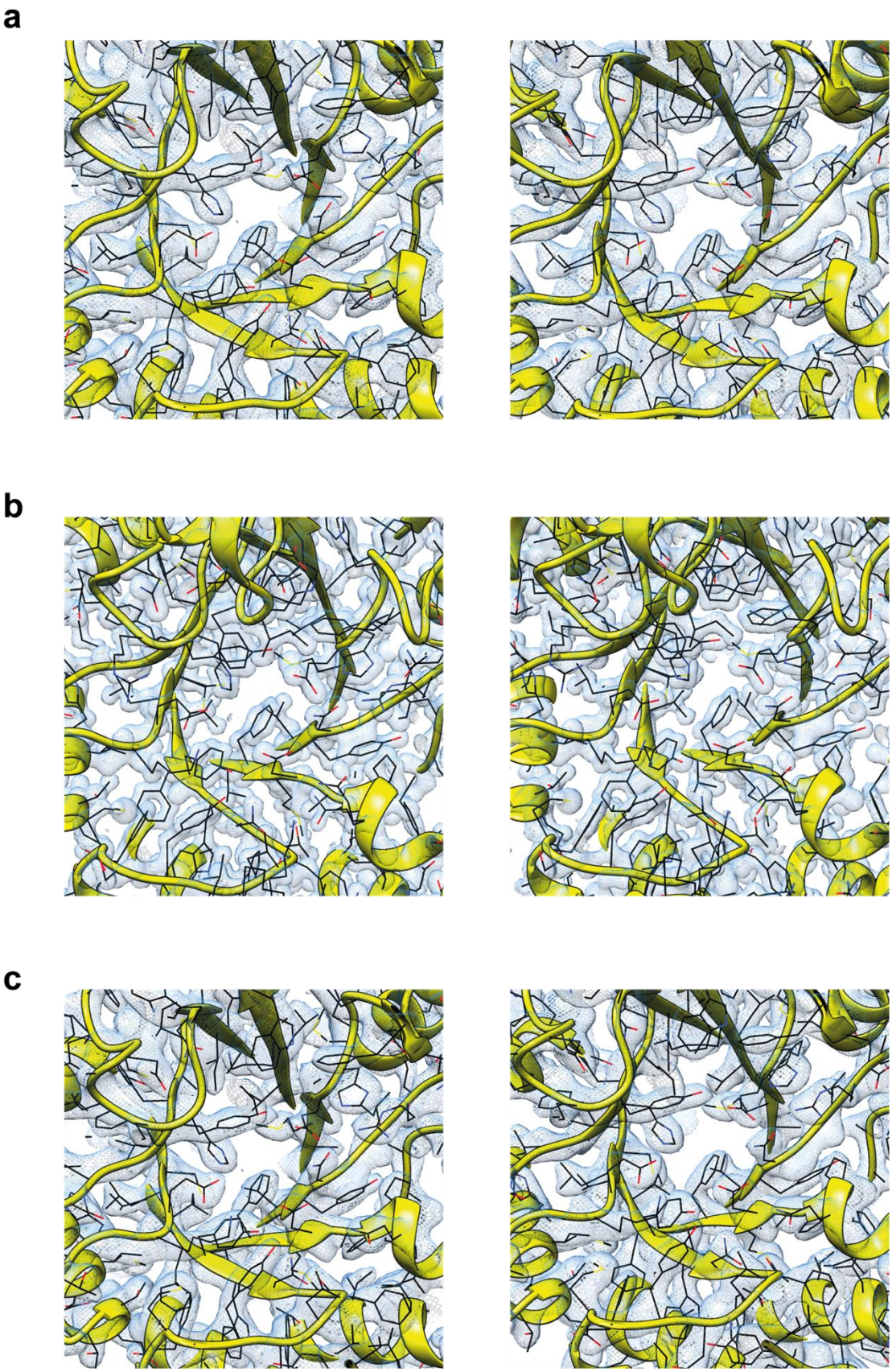

Supplementary Fig. 11 | Electron density maps of the refined PbFucA X-ray crystal structures. Final electron density maps (2mFo-Dfc contoured at 1σ) corresponding to PbFucA-1 (PDB code 8RG3) (**a**), PbFucA-2 (PDB code 8RG4) (**b**) and PbFucA-3 (PDB code 8RG4) (**c**).

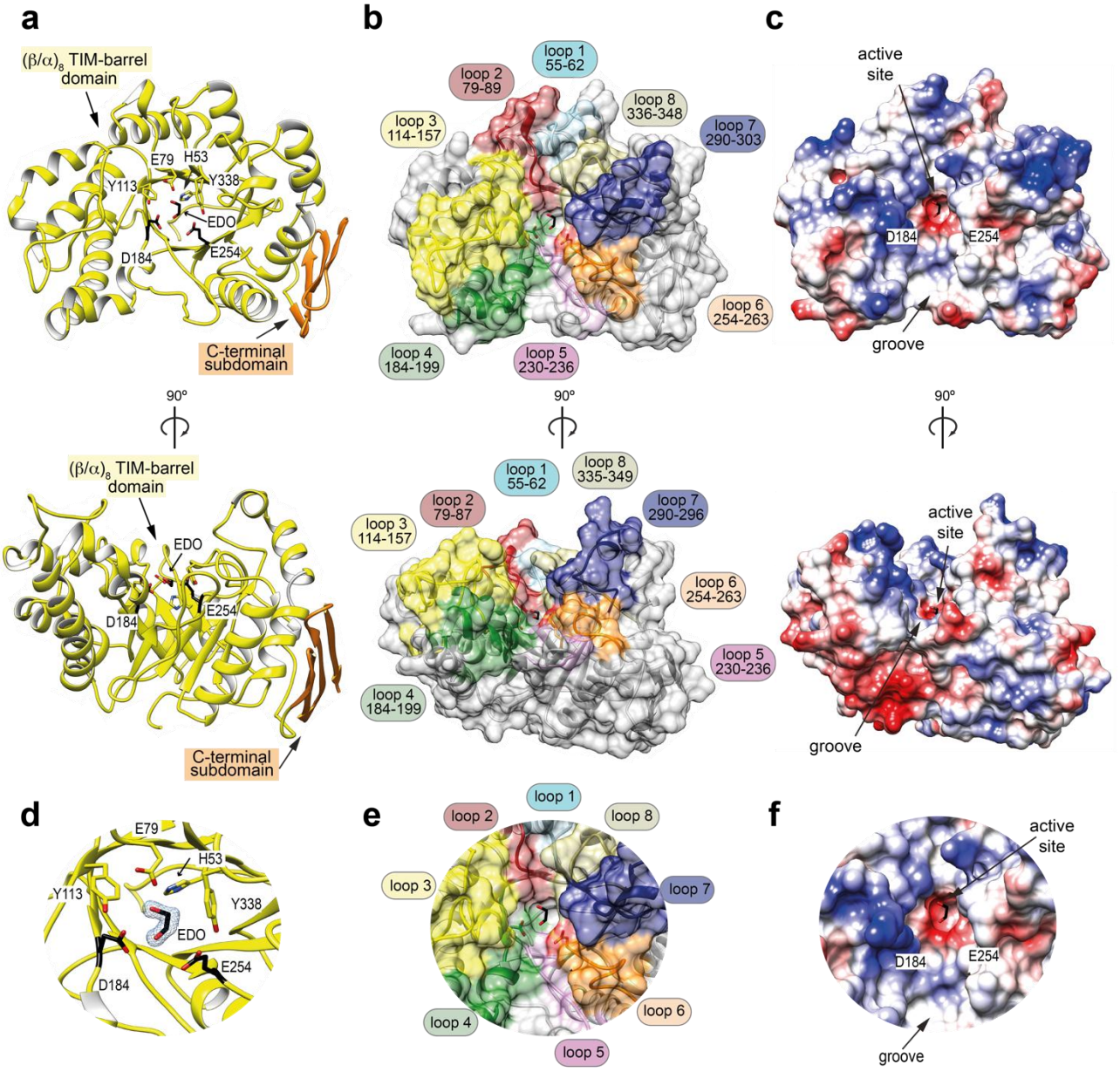

Supplementary Fig. 12 | The overall structure of PbFucA. a Two cartoon representations showing the general fold and secondary structure organization of PbFucA. Domains, catalytic residues, and residues interacting with the glycerol molecule are annotated. **b** Two surface representations of the PbFucA. Loops that form the main groove of PbFucA are highlighted in different colors. **c** Two electrostatic surface representations of PbFucA showing the location of the catalytic site. **d-f** Close-up view of the active site of the catalytic site of PbFucA shown as cartoon/stick and the electron density map of ethylene glycol (EDO) shown at 1.0 σ r.m.s.d (**d**), with annotated loops (**e**), and as electrostatic surface representation (**f**).

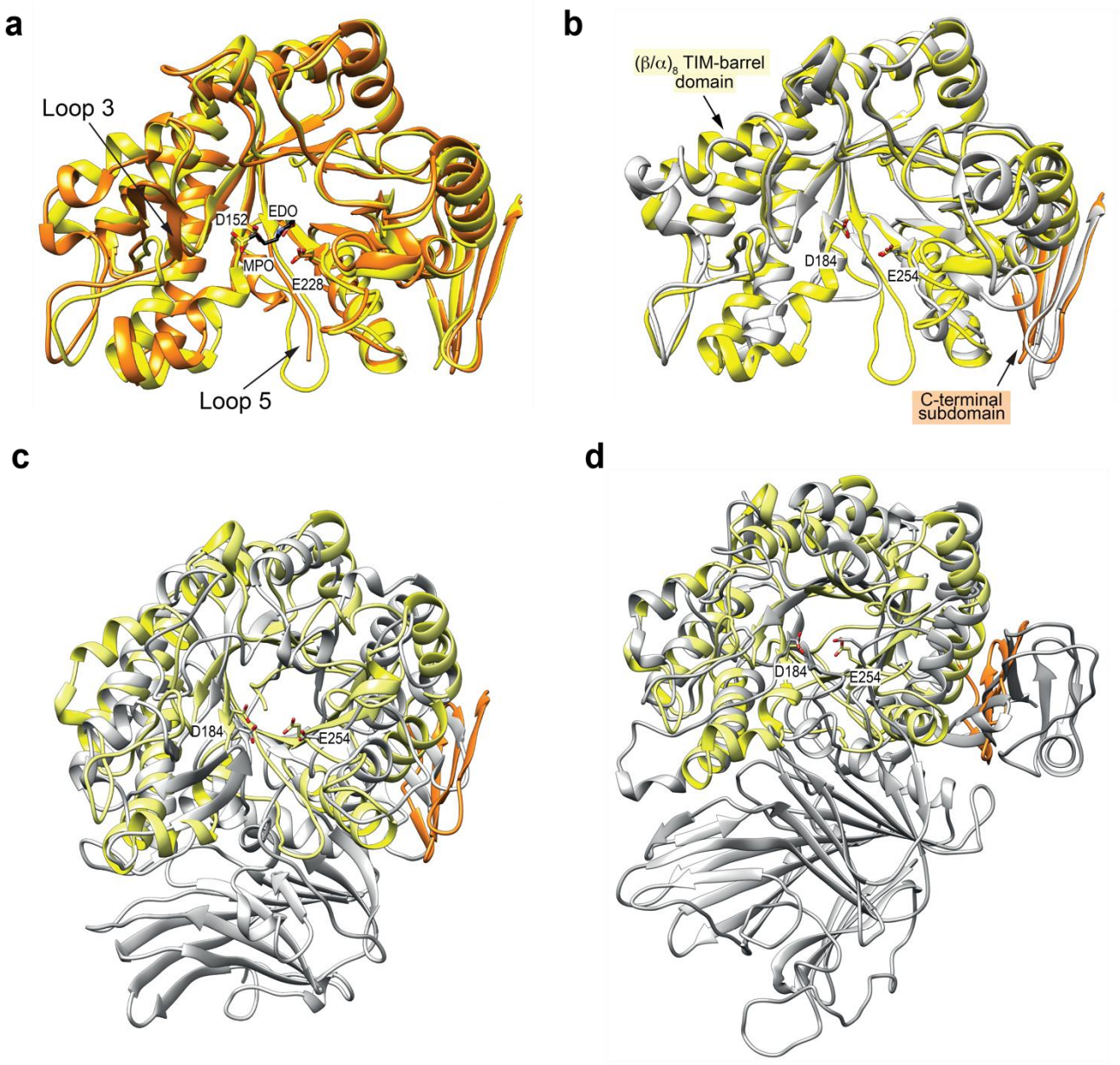

Supplementary Fig. 13 | Structural homology analysis of Rho5174 and PbFucA. a Superposition of X-ray crystal structures of Rho5174 (PDB code 9F9V) and PbFucA (PDB code 8RG4). Catalytic residues of Rho5174 are highlighted. **b-d** Superposition of the *Pb*FucA-2 crystal structure and Fun168A (**b**), an endo-a-1,3-fucoidanase from *W. funcanilytica* CZ1127T, *Tm*GalA (**c**), α-galactosidase from *Thermotoga maritima* (PDB code 5M1I; GH36, grey), and LaMel36A (**d**), α-galactosidase from *Lactobacillus acidophilus* (PDB code 2XN1; GH36, grey). The $(\beta/\alpha)_8$-TIM barrel and C-terminal subdomain are colored yellow and orange, respectively.

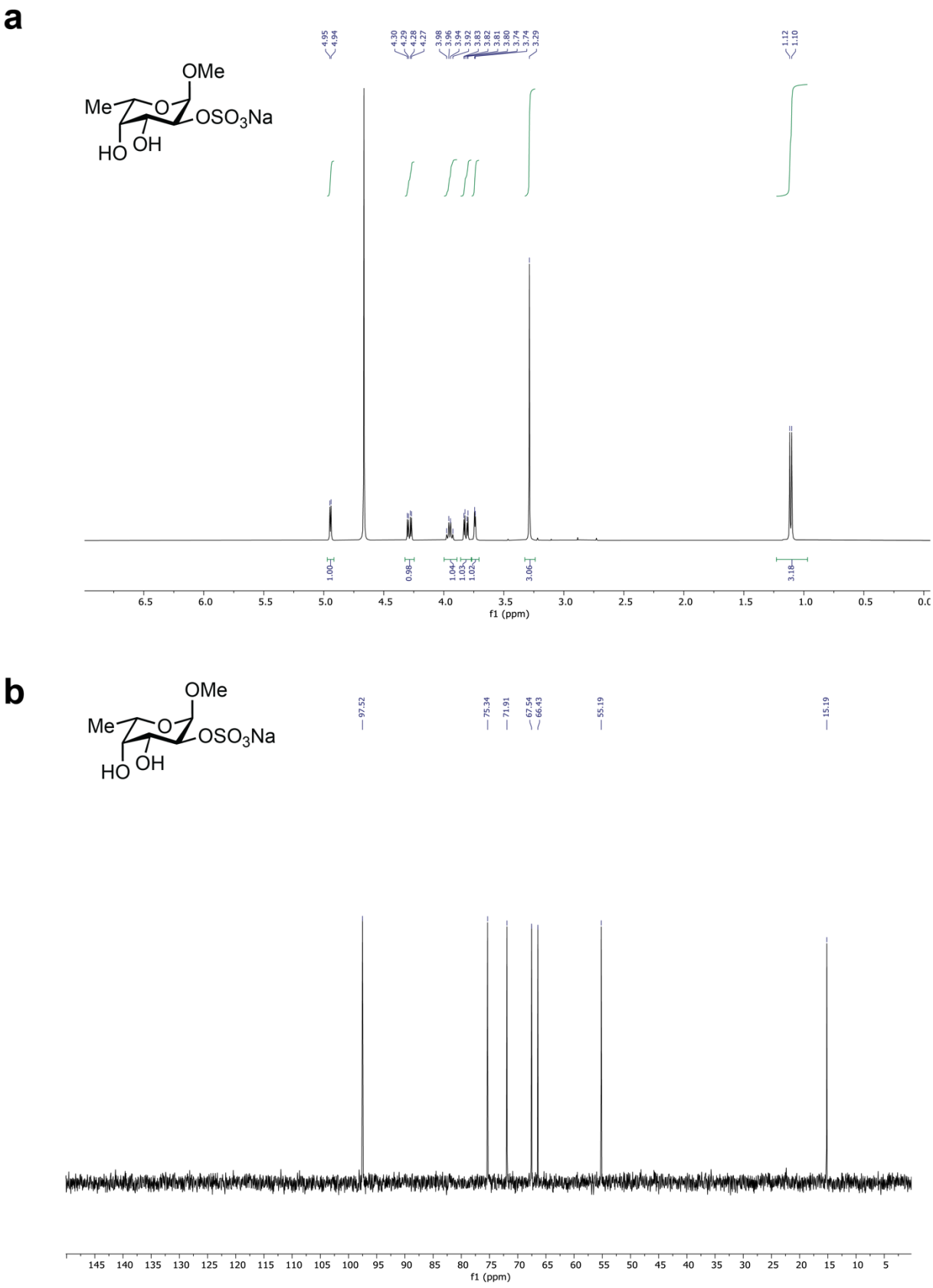

Supplementary Fig. 14 | NMR spectra of sodium methyl-α-L-fucopyranoside 2-sulfate (Fuc2SO$_4$). **a** ^{1}**H NMR** (400 MHz, D_2O) δ 4.94 (d, *J* = 4.9 Hz, 1H), 4.29 (dd, *J* = 10.4 Hz, *J* = 3.9 Hz, 1H), 3.95 (m, 1H), 3.82 (dd, *J* = 10.4 Hz, *J* = 3.4 Hz, 1H), 3.74 (d, J = 3.4 Hz, 1H), 3.29 (s, 3H), 1.11 (d, *J* = 6.7 Hz, 3H). **b** ^{13}**C NMR (**100 MHz, D_2O) δ 97.5, 75.3, 71.9, 67.5, 66.4, 55.2, 15.2. **HRMS (ESI)** calcd for $C_7H_{13}O_8S$ [M^-]: 257.0337, found: 257.0347

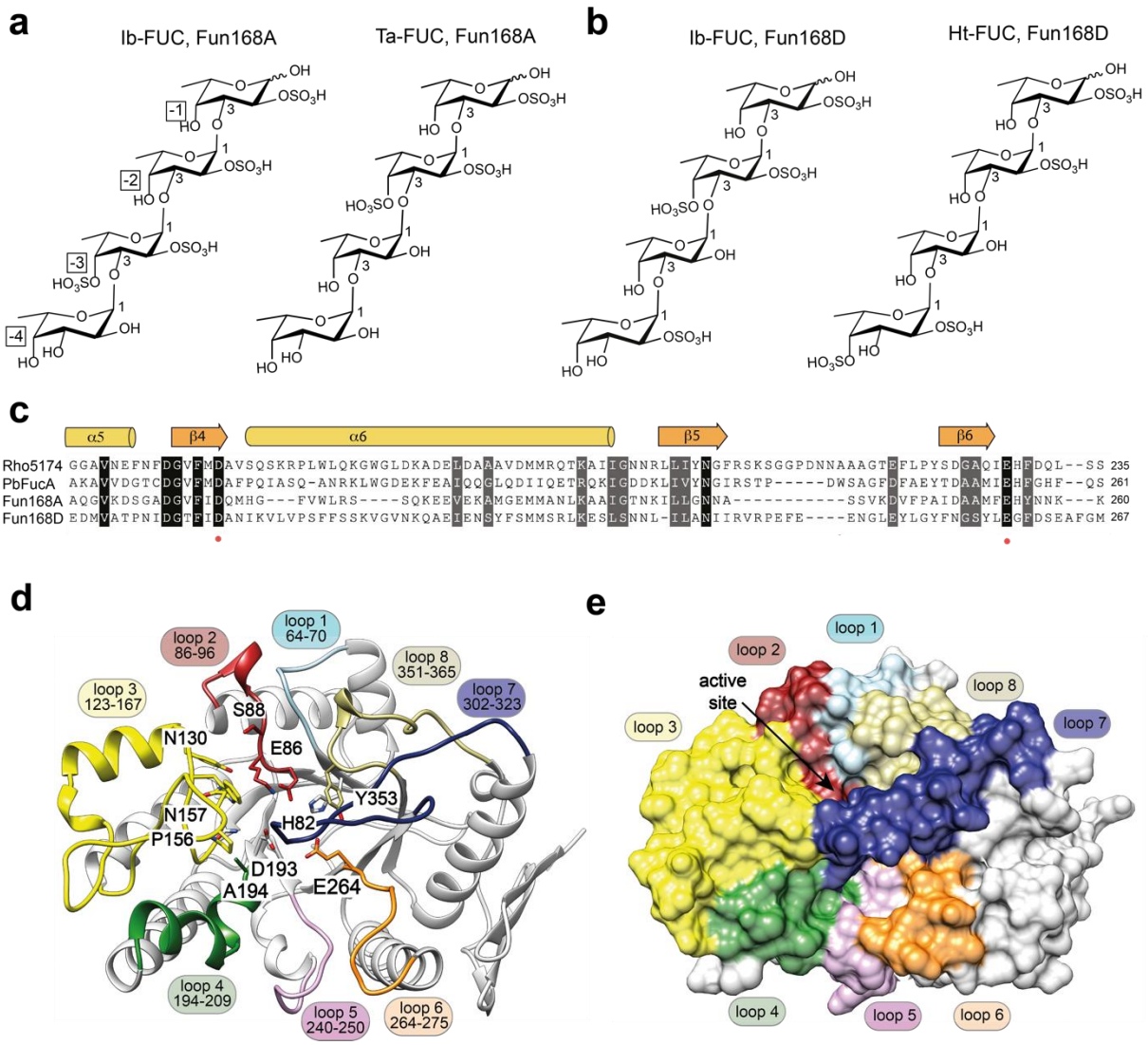

Supplementary Fig. 15 | Sequence alignment of Rho5174, PbFucA, Fun168A and Fun168D. a Chemical structures of sulfated tetrasaccharides, products of the reaction between fucoidan from *I. badionotus* and *T. ananas* and Fun168A. **b** Chemical structures of sulfated tetrasaccharides, products of the reaction between fucoidan from *I. badionotus* and *T. ananas* and Fun168D. **c** Sequence alignment of a selected region of Rho5174, PbFucA, Fun168A and Fun168D, showing the conservation of key residues in the catalytic site. **d** Cartoon representation of the Alphafold model of Fun168D showing the general fold and secondary. **e** Surface representation of the Alphafold model of Fun168D.

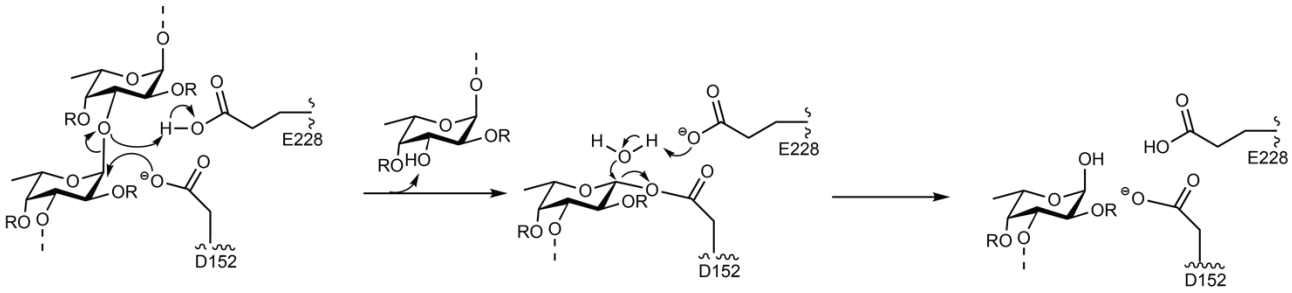

Supplementary Fig. 16 | Proposed catalytic mechanism of Rho5174. In the first step, D152 of Rho5174 acts as a nucleophile attacking the anomeric center to form a glycosyl-enzyme intermediate. In the second step, E228 of Rho5174 acts as a base deprotonating a water molecule that hydrolyzes the glycosidic bond, leading to the regeneration of the sugar with retention of the anomeric configuration.

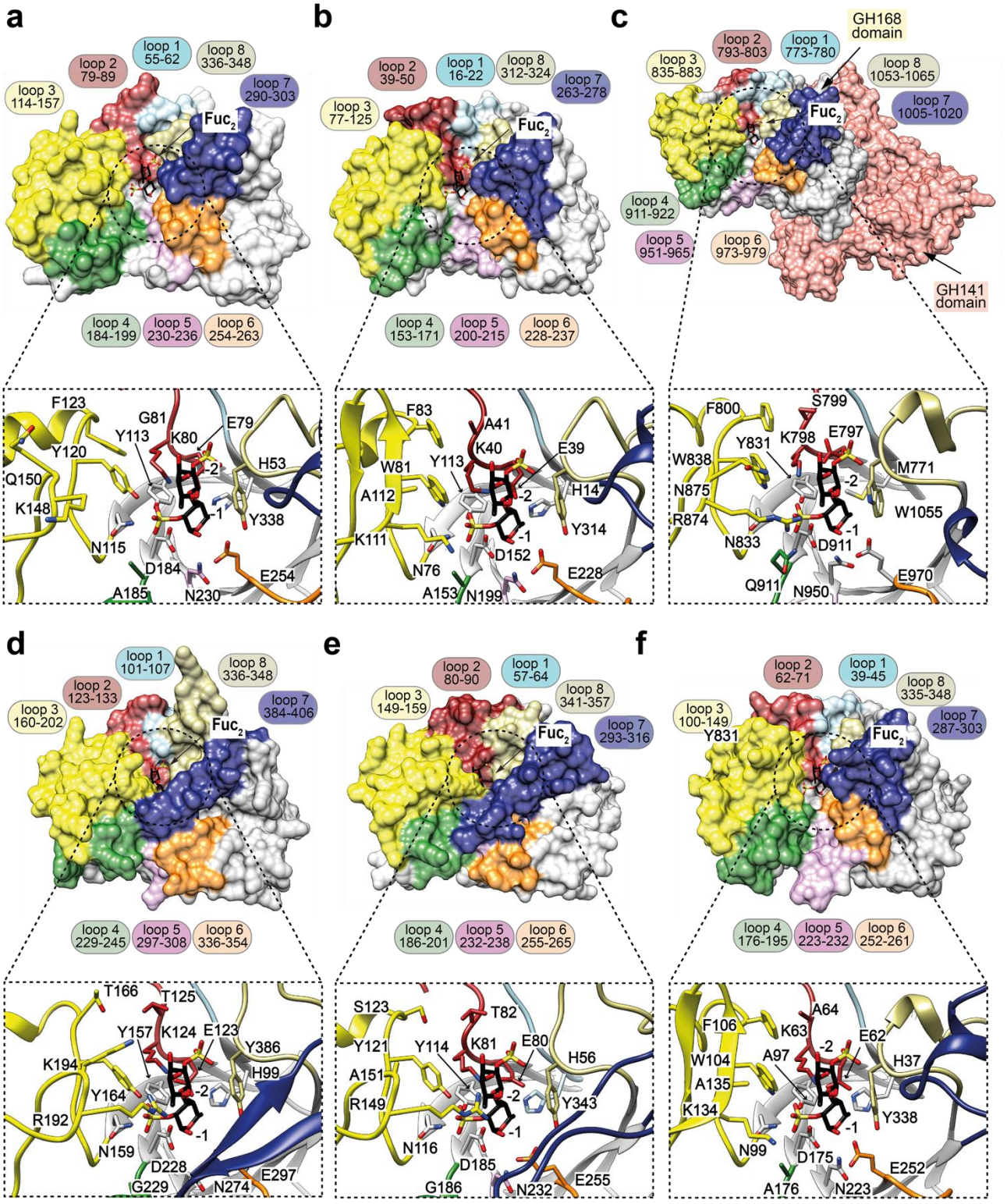

Supplementary Fig. 17 | Structural comparison of Rho5174 and *Pb*FucA with GH168 enzymes from strains 892 and 913. a-f Surface representation of the X-ray crystal structures of PbFucA (**a**) and Rho5174 (**b**) and the Alphafold predicted structures of 892_06282 (**c**), 892_06289 (**d**), 913_01189 (**e**) and 913_05635 (**f**). The loops are highlighted in different colours. The Fuc (-1) and Fuc (-2) of Ib-FUC (Fuc_2) found in the active site of the crystal structure of Fun168A (PDB code 8YA7) are superimposed in each structure.

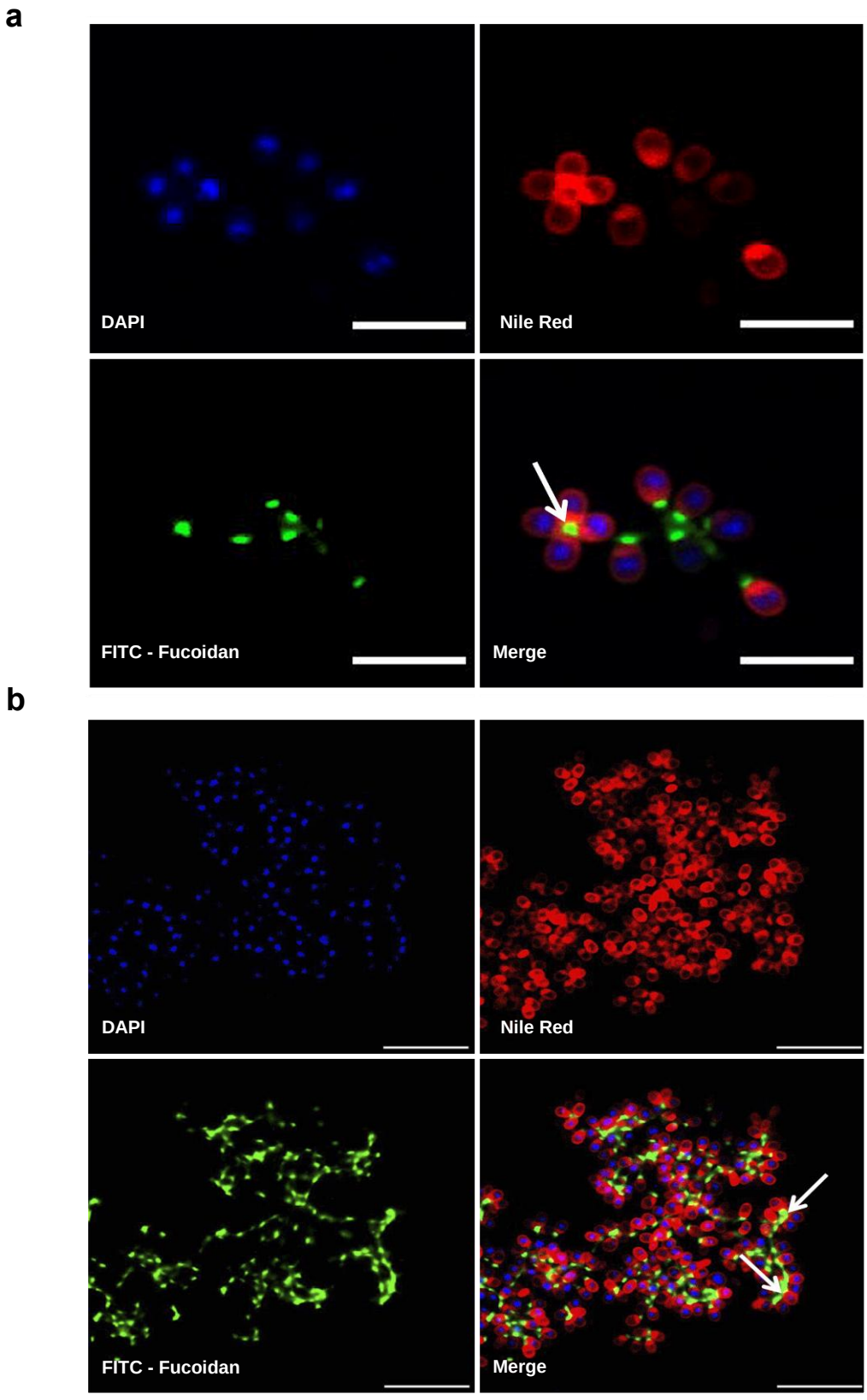

Supplementary Fig. 18 I FITC-Fucoidan visualization in contact with *Planctomycetota* strain 913. Strain 913 was grown in the presence of FITC-Fucoidan (0.05%) fixed and visualized by confocal microscopy. Bacterial cellular envelope and nucleoid region were labeled using Nile Red (3 µg ml^{-1}) and DAPI (1 µg ml^{-1}), respectively. Scale bar = 10 µm. The white arrow marks fucoidan bound to several 913 bacteria, forming a rosette-like structure (a) or along FITC-Fucoidan fibers (b). Representative image of n = 3 independent experiments.

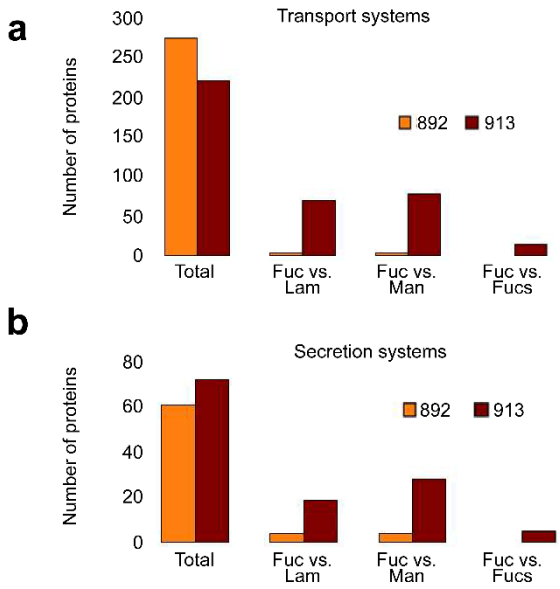

Supplementary Fig. 19 I Total number of proteins related to transport (a) and secretion systems (b) in the genomes of strains 892 and 913 (total) or induced by growth on fucoidan from *Fucus vesiculosus* vs. laminarin, mannose and fucose.

4. Supplementary References

1. Sichert, A. *et al.* Ion-exchange purification and structural characterization of five sulfated fucoidans from brown algae. *Glycobiology* **31**, 352–357 (2021).
2. Zueva, A. O. *et al.* Production of high- and low-molecular weight fucoidan fragments with defined sulfation patterns and heightened in vitro anticancer activity against TNBC cells using novel endo-fucanases of the GH107 family. *Carbohydr. Polym.* **318**, 121128 (2023).
3. Lu, J. *et al.* Fucoidan Extracted from the New Zealand Undaria pinnatifida—Physicochemical Comparison against Five Other Fucoidans: Unique Low Molecular Weight Fraction Bioactivity in Breast Cancer Cell Lines. *Mar. Drugs* **16**, 461 (2018).
4. Vaamonde-García, C. *et al.* Study of fucoidans as natural biomolecules for therapeutical applications in osteoarthritis. *Carbohydr. Polym.* **258**, 117692 (2021).
5. Koh, H. S. A., Lu, J. & Zhou, W. Structure characterization and antioxidant activity of fucoidan isolated from Undaria pinnatifida grown in New Zealand. *Carbohydr. Polym.* **212**, 178–185 (2019).
6. Liu, Y. *et al.* Substrate Use Prioritization by a Coculture of Five Species of Gut Bacteria Fed Mixtures of Arabinoxylan, Xyloglucan, β-Glucan, and Pectin. *Appl. Environ. Microbiol.* **86**, e01905-19 (2020).
7. Shen, J., Chang, Y., Zhang, Y., Mei, X. & Xue, C. Discovery and Characterization of an Endo-1,3-Fucanase From Marine Bacterium Wenyingzhuangia fucanilytica: A Novel Glycoside Hydrolase Family. *Front. Microbiol.* **11**, 1–11 (2020).
8. Shen, J. *et al.* Characterization of a novel endo-1,3-fucanase from marine bacterium Wenyingzhuangia fucanilytica reveals the presence of diversity within glycoside hydrolase family 168. *Carbohydr. Polym.* **318**, 121104 (2023).
9. Holm, L. Using Dali for Protein Structure Comparison. in *Methods in Molecular Biology* vol. 2112 29–42 (Humana Press Inc., 2020).
10. Adamson, C. *et al.* Structural Snapshots for Mechanism-Based Inactivation of a Glycoside Hydrolase by Cyclopropyl Carbasugars. *Angew. Chemie - Int. Ed.* **55**, 14978–14982 (2016).
11. Fredslund, F. *et al.* Crystal structure of α-galactosidase from lactobacillus acidophilus NCFM: Insight into tetramer formation and substrate binding. *J. Mol. Biol.* **412**, 466–480 (2011).
12. Paoli, L. *et al.* Biosynthetic potential of the global ocean microbiome. *Nature* **607**, 111–118 (2022).
13. Anso, I. *et al.* Turning universal O into rare Bombay type blood. *Nat. Commun.* **14**, 1765 (2023).